BIOORGANIC CHEMISTRY 15, 31–42 (1987)

Application of Linear Free-Energy Relationships to the Mechanistic Probing of Nonenzymatic and NAD$^+$-Glycohydrolase-Catalyzed Hydrolysis of Pyridine Dinucleotides

CÉLINE TARNUS AND FRANCIS SCHUBER[1]

Laboratoire de Chimie Enzymatique (UA 570), Institut de Botanique, 28, rue Goethe, 67000-Strasbourg, France

Received May 19, 1986

The use of NAD$^+$ analogs lacking a carbonyl function at position C-3 of the pyridinium moiety allowed the manipulation of the kinetic mechanism of calf spleen NAD$^+$ glycohydrolase so as to render the cleavage of the pyridinium–ribose bond rate limiting. The analogs used in this study are relatively poor substrates of the enzyme. They present an affinity for the active site which is independent of the nature of their substituent (K_i = 10 ± 2 μM), suggesting that the specificity of the NAD$^+$ glycohydrolase reflects the dynamic steps occurring after the formation of the Michaelis complex. The maximal rates of hydrolysis of the NAD$^+$ analogs are very sensitive to the pK_a of the departing pyridine; a Brönsted plot (r = 0.99) gave a $\beta_{lg} = -0.90$ (at 37°C). From this plot we could estimate that for NAD$^+$, the specific interaction of the 3-carboxamide group with the active site contributed to the catalysis by decreasing the energy barrier by about 2 kcal mol^{-1}. We have also studied the nonenzymatic hydrolysis of NAD$^+$ and its analogs under conditions (pH-independent hydrolysis) which favor a unimolecular mechanism. In this case a linear Brönsted plot was also found (r = 0.99) with $\beta_{lg} = -1.11$ (at 37°C). Our data indicate that NAD$^+$ glycohydrolase catalyzes the chemical cleavage of the pyridinium–ribose bond, over a 10^3 rate difference, according to a single mechanism involving a late transition state in which the scissile bond is broken. The present study strongly supports our previous hypothesis (F. Schuber, P. Travo, and M. Pascal (1979) *Bioorg. Chem.* **8,** 83) according to which NAD$^+$ glycohydrolase catalyses unimolecular decomposition of its substrates with generation of an ADP–ribosyl oxocarbonium ion intermediate which must be stabilized by the active site of the enzyme.

INTRODUCTION

NAD$^+$ glycohydrolase (EC 3.2.2.6)[2] catalyzes the hydrolytic cleavage of the nicotinamide–ribose bond in NAD(P)$^+$ and transglycosidation reactions which allow facile synthesis of pyridinium analogs of NAD$^+$ (*1*). The mechanism of the

[1] To whom correspondence should be addressed.

[2] Abbreviations used: NAD$^+$ase or NAD$^+$ glycohydrolase, NAD(P)$^+$ nucleosidase; iNAD$^+$, isonicotinamide adenine dinucleotide; isNAD$^+$, isothionicotinamide adenine dinucleotide; PdAD$^+$, pyridine adenine dinucleotide; Br^{4}PdAD$^+$, 4-bromopyridine adenine dinucleotide; ((3,4-CH_3)$_2$)PdAD$^+$, 3,4-dimethylpyridine adenine dinucleotide; cn^{4}PdAD$^+$, 4-cyanopyridine adenine dinucleotide; f^{4}PdAD$^+$, 4-formylpyridine adenine dinucleotide; hy^{4}PdAD$^+$, 4-carboxyhydrazidepyridine adenine dinucleotide; n^{3}PdAD$^+$, 3-aminopyridine adenine dinucleotide; HPLC, high-pressure liquid chromatography.

0045-2068/87 $3.00

enzyme of mammalian origin has been studied by several groups (*2–5*). Steady-state kinetics have indicated that the minimum kinetic mechanism was ordered uni-bi, the formation of an intermediary E·ADP–ribosyl complex, which occurs after the departure of nicotinamide, being rate limiting (*6*). This intermediate can react with acceptors such as water, methanol (*7*), or pyridines (*8*) with retention of configuration. In order to explain at a molecular level how NAD^+ glycohydrolase catalyses the hydrolysis of the N-glycosidic bond it was important to provide some information on the nature of the chemical step(s) leading to the E·ADP–ribosyl complex. A likely mechanism consists of unimolecular decomposition of the substrate which generates an intermediate possessing characteristics of an oxocarbonium ion (*4, 5*). However, it is now evident that such reactions, depending on the stability of the intermediate and on its stabilization by the enzyme, often follow pathways which represent a borderline between "classical" S_N1 and S_N2 mechanisms (*9*). In an attempt to determine the influence of the leaving ability of the pyridinium moieties in NAD^+ analogs on the rate of hydrolysis catalyzed by calf spleen NAD^+ glycohydrolase, we found that the enzyme presented a kinetic specificity. Only the analogs possessing a carbonyl function at position C-3 were good substrates; the other analogs, regardless of the energy of their pyridinium–ribose bond, were poorly hydrolyzed but behaved as potent competitive inhibitors (*5*). We concluded that the rate-limiting step of the hydrolysis of NAD^+ catalyzed by the enzyme was more complex than a simple chemical reaction and could involve an additional step such as a slow transconformation following substrate binding, leading to the destabilization of the scissile bond (*5*). Such a hypothesis was strengthened by the results of Cordes' group concerning α-secondary deuterium kinetic isotope effects (*4*). No isotope effect was measurable for the hydrolysis of NAD^+ catalyzed by pig brain NAD^+ glycohydrolase. In contrast, a poor substrate such as NMN^+ was hydrolyzed with a secondary isotope effect comparable to that found in nonenzymatic hydrolysis under pH conditions favoring unimolecular decomposition. The authors concluded that both NAD^+ and NMN^+ were hydrolyzed enzymatically according to a dissociative mechanism, i.e., via the formation of a transient oxocarbonium ion, the chemical step in the case of NAD^+ not being rate limiting. Since this work it became evident, however, that in substitution reactions where the reactive center is adjacent to electron-donating atoms, α-secondary deuterium kinetic isotope effects cannot be safely used to distinguish between concerted and dissociative reaction pathways (*10–12*). Therefore additional information was needed to approach the chemical nature of the reaction catalyzed by the NAD^+ glycohydrolase. In the present study we have applied linear free-energy relationships (*13*) to the mechanistic probing of NAD^+ glycohydrolase.

Alteration of enzymatic reaction conditions, such as by changing the pH or by the use of allosteric activators, can influence relative rates leading to the bond-breaking step and hence modulate the expression of kinetic isotope effects (*14, 15*). Such a strategy can also be successful using poor substrates, e.g., NMN^+ in the case of NAD^+ glycohydrolase (*4*). We reasoned that pyridinium analogs of NAD^+ which are poor substrates, i.e., analogs that lack a carbonyl function at C-3

of the pyridinium moiety, might be useful to circumvent the slow conformational step observed in the case of the hydrolysis of NAD^+. If such analogs are indeed hydrolyzed, the rate-limiting step might then reflect the chemical N-glycosidic bond cleavage and be sensitive to the pK_a of the departing pyridine. The access to large quantities of calf spleen NAD^+ glycohydrolase and reaction monitoring by HPLC allowed us to perform such experiments. We found that pyridinium analogs of NAD^+ are indeed hydrolyzed, albeit slowly, by the enzyme at rates which are very sensitive to the energy of the pyridinium–ribose bond. Similarly we have studied the nonenzymatic hydrolysis of NAD^+ and analogs under unimolecular rate conditions. Comparison of the data gives new insight into the mechanism of the NAD^+ glycohydrolase-catalyzed reactions.

EXPERIMENTAL

β-NAD^+, α-NAD^+, and β-NMN^+ were obtained from Sigma Chemical Co. The free pyridines used in the analog synthesis were Fluka products. The following analogs were prepared according to published procedures: $PdAD^+$ (*16*), hy^4PdAD^+ (*17*) and n^3PdAD^+ (*18*). Br^4PdAD^+, $((3,4\text{-}CH_3)_2)PdAD^+$, f^4PdAD^+, $iNAD^+$, and $isNAD^+$ were synthesized from NAD^+ by the standard pyridine base-exchange reaction catalyzed by pig brain NAD^+ glycohydrolase (*2*). The analogs were purified by ion-exchange chromatography on a Dowex 1-X2 (formate form) column (*19*); any residual NAD^+ contaminating the analog fraction was eliminated either by enzymatic cleavage with *Neurospora crassa* NAD^+ glycohydrolase (*20*) or by conversion into NADH by alcohol dehydrogenase and subsequent degradation in acidic media (*21*). After a final chromatography the analogs were obtained with a purity superior to 98% as judged by HPLC analysis. cn^4PdAD^+ was obtained in quantitative yield from $isNAD^+$ by treatment with silver nitrate, as described before (*22*).

Neurospora crassa and pig brain NAD^+ glycohydrolases and yeast alcohol dehydrogenase were purchased from Sigma Chemical Co. NAD^+ glycohydrolase used for the kinetic studies was solubilized with detergent (Emulphogene BC-720) from calf spleen microsomes as described previously (*23*). The purification of this form of the enzyme will be reported elsewhere (H. M. Muller *et al.*), its specific activity was about 20 units/mg protein.

Reaction progress and product purity were determined by HPLC by use of a Waters Co. modular system. Chromatography was carried out on a 3.9 × 300-mm μBondapak C_{18} column (Waters) operated at ambient temperature, pressures of 1000–1500 psi and flow rate of 1 ml/min. The compounds were isocratically eluted with 10 mM $(NH_4)H_2PO_4$ in acetonitrile–water (5 : 95) at pH 5.5 (*24*) and detected at 260 nm. Peaks were identified by retention time and areas were integrated (Spectra Physics, Model SP 4270) for quantitative analysis. These chromatography conditions allowed an excellent separation of the NAD^+ analogs from their hydrolytic products, i.e., the free pyridines, ADP–ribose, AMP, and adenosine.

Kinetic Measurements

Enzymatic hydrolysis of NAD$^+$ and analogs. The hydrolysis of NAD$^+$ and its pyridinium analogs (final concentration 600 μM) was carried out at 37°C in 50 mM sodium phosphate buffer, pH 7.4, containing 0.1% (w/v) Emulphogene BC-720 (final volume 1 ml) in the presence of varying concentrations of calf spleen NAD$^+$ glycohydrolase. Reaction progress was analyzed by HPLC on aliquots and k_{obs}, the observed rate of substrate hydrolysis, was obtained (least-squares analysis) from the slope of the progress curve, i.e., ADP–ribose formation with time. The rates of hydrolysis of the different analogs are expressed as relative rates (NAD$^+$ = 1), i.e., $V_{rel} = k_{obs}$/NADase units. Under these experimental conditions no spontaneous decomposition of the dinucleotides or of ADP–ribose was observed; the enzyme-catalyzed hydrolysis was linear with time for at least 50% of substrate conversion and the observed rates were proportional to the enzyme concentration. In some cases initial rates of hydrolysis were determined using a titrimetric method according to the conditions described previously (*25*). The kinetic parameters (V, K_m (app)) were calculated according to Wilkinson (*26*). Inhibition constants were determined at fixed inhibitor concentrations with varying NAD$^+$ concentrations (Lineweaver–Burk plots).

Nonenzymatic hydrolysis of NAD$^+$ and analogs. Monomolecular decomposition of NAD$^+$ and its analogs (final concentration 1 mM) was studied in 50 mM sodium phosphate buffer, pH 6.4, containing 0.5 M NaCl (total volume 1 ml) at temperatures varying from 65 to 120°C (thermostated oil bath, $t \pm 0.5$°C). Aliquots were analyzed at different times by HPLC. In contrast to enzymatic hydrolysis where the reaction products were stable, under the present reaction conditions, e.g., when the incubation time at 100°C was superior to 90 min, ADP–ribose was converted successively into AMP and adenosine. Pyridine dinucleotides hydrolysis was therefore followed by monitoring the reactant peak disappearance, using adenine added at time zero as the internal standard. The observed rates were calculated using a least-squares program.

RESULTS

Hydrolysis of NAD$^+$ Analogs by NAD$^+$ Glycohydrolase

Because pyridinium analogs of NAD$^+$ possessing a carbonyl function at position C-3 proved to be fairly good substrates of calf spleen NAD$^+$ glycohydrolase (*5*), we synthesized analogs which have this function at C-4, e.g., iNAD$^+$, f^{4}PdAD$^+$, and hy^{4}PdAD$^+$, or which have different substituents at C-3 or C-4, e.g., cn^{4}PdAD$^+$, PdAD$^+$, ((3,4-CH_3)$_2$)PdAD$^+$, and n^{3}PdAD$^+$; such analogs should be poorer substrates of the enzyme (*5*). These pseudosubstrates were all potent competitive inhibitors of NAD$^+$ glycohydrolase; their K_i values were very similar, i.e., 10 $\pm$ 2 μM, compared to the K_m (60 μM) of NAD$^+$. Using large amounts of enzyme, we were able to demonstrate that these NAD$^+$ analogs could be hydrolyzed by NAD$^+$ glycohydrolase, albeit at much slower rates than NAD$^+$. The

TABLE 1

RELATIVE RATES OF HYDROLYSIS OF NAD+ AND ITS PYRIDINIUM ANALOGS CATALYZED BY CALF SPLEEN NAD+ GLYCOHYDROLASE[a]

Substrate	Substituent	Relative rate[b] (nmol min^{-1} U^{-1})	pK_a[c]
cn^{4}PdAD$^+$	-CN	650	2.14
NAD$^+$	$-CONH_2$	1000	3.33
NMN$^+$	$-CONH_2$	198	3.33
hy^{4}PdAD$^+$	$-CONHNH_2$	13.2	3.58
iNAD$^+$	$-CONH_2$	25.2	3.87
Br^{4}PdAD$^+$	-Br	20.4	3.96
f^{4}PdAD$^+$	-CHO	5.0	4.72
PdAD$^+$	-H	2.0	5.23
n^{3}PdAD$^+$	$-NH_2$	0.17	5.98

[a] Determined in 50 mM sodium phosphate buffer at pH 7.4, 37°C, using 600 μM substrate.

[b] One unit is defined as the amount of NAD+ase catalyzing the hydrolysis of 1 μmol NAD+/min under the conditions defined above.

[c] pK_a of the parent pyridinium ion (*27, 28*).

reaction progress of pyridinium–ribose bond cleavage was followed by an HPLC method (*24*) which allows fast and easy separation of substrates from reaction products, i.e., ADP–ribose and the parent free pyridine. The relative rates of the enzyme-catalyzed hydrolysis of the analogs are given in Table 1 along with the pK_a of the leaving pyridines. Because the substrate concentration used in these rate determinations (i.e., 600 μM) was saturating, the given rates correspond to relative maximal rates. Table 1 also presents data for the hydrolysis of β-NMN$^+$; this mononucleotide (K_m = 1.3 mM) is hydrolyzed fivefold slower (V_{max}) than NAD$^+$ by calf spleen NAD$^+$ glycohydrolase. It was shown by Cordes' group to be cleaved enzymatically, in contrast to NAD$^+$, with a measurable secondary deuterium kinetic isotope effect (*4*). The representation of the logarithms of the relative hydrolysis rates versus the pK_a of the leaving pyridines according to Brönsted is given in Fig. 1. A linear plot is obtained for the NAD$^+$ analogs over 4 pK_a units: $\log k = -0.90pK_a + 4.83$ ($r = 0.99$). The slope $\beta_{lg} = -0.9$ reveals a high sensitivity of the reaction catalyzed by the NAD$^+$ glycohydrolase to the pK_a of the leaving pyridine. Alternatively the rates were plotted according to Hammett, using σ_m and σ_p as substituent constants. A linear plot was obtained: $\log k = 4.41\sigma + 0.16$ (r = 0.98) with a slope $\rho = 4.41$ (not shown). In agreement with our earlier work (*5*), NAD$^+$ is more susceptible to hydrolysis than expected from the pK_a of nicotinamide. Interpolation from the Brönsted plot allows one to calculate that the presence of a carboxamide group at position 3 of the pyridinium moiety of NAD$^+$ results in a rate advantage of 14 (this number amounts to 40 when determined from Hammett plot). Similarly, β-NMN$^+$ was hydrolyzed faster, i.e., 2.8- and 8-fold

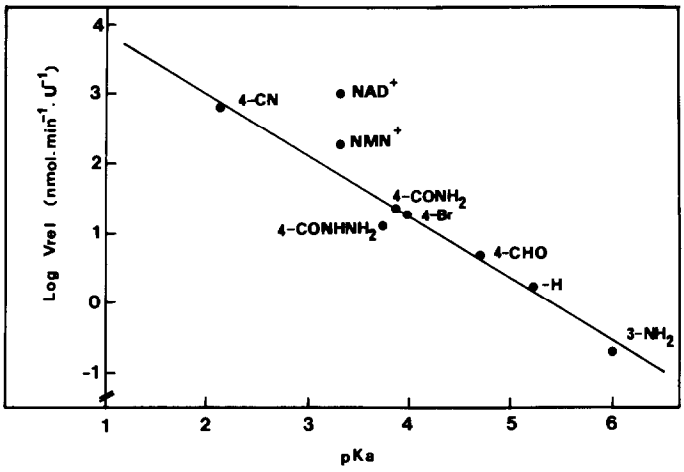

FIG. 1. Brönsted plot of the calf spleen NAD^+ glycohydrolase-catalyzed hydrolysis rates of pyridinium analogs of NAD^+. Relative maximal rates of hydrolysis, as defined in Table 1, determined in a 50 mM sodium phosphate buffer, pH 7.4, at 37°C, are plotted against the pK_a of the leaving pyridine bearing varying substituents at position 3 or 4. NAD^+ and NMN^+ hydrolysis rates are given for comparison.

deduced, respectively, from Brönsted and Hammett plots, than expected from the energy of its scissile bond. hy^4PdAD^+ is hydrolyzed somewhat less efficiently by the enzyme than predicted; in this respect it might be worthwhile to mention that calf spleen NAD^+ glycohydrolase belongs to the "isonicotinic acid hydrazide (INH)-sensitive" NADases; i.e., the enzyme is efficiently inhibited by INH, but is unable to catalyze the formation of hy^4PdAD^+ (*17*).

Nonenzymatic Hydrolysis of NAD^+ and Analogs

NAD^+ undergoes pH-independent and specific base-catalyzed hydrolysis to yield nicotinamide and ADP–ribose (*29, 30*). The pH-independent reaction, which occurs between pH 2 and 7, shows little sensitivity to buffer concentration (*31*). This unimolecular decomposition, because of the magnitude of the kinetic α-secondary isotope effect, is thought to generate an ADP–ribosyl oxocarbonium ion intermediate in the rate-limiting step (*4*). We have determined the rate of unimolecular decomposition of NAD^+ and its pyridinium analogs at pH 6.4 (Table 2) in a phosphate buffer. This buffer was shown previously to not participate per se in the reaction and conveniently its pH changes minimally with temperature (*30*). The hydrolysis of the pyridine dinucleotides was monitored by HPLC which was ideally suited to follow the appearance of the reaction products. Interestingly under our experimental conditions, even for $((3,4\text{-}CH_3)_2)PdAD^+$, i.e., the analog studied whose leaving pyridine had the highest pK_a, the pyridinium–ribose linkage was always the first one to be cleaved. Indeed, the rates of AMP and adenosine appearance, as analyzed by HPLC, showed that they originated from ADP–ribose, the first reaction product of hydrolysis of the NAD^+ analogs. Hydrolysis of the different analogs followed perfect pseudo-first-order kinetics for at least

TABLE 2

FIRST-ORDER RATE CONSTANTS OF NONENZYMATIC HYDROLYSIS OF NAD+ AND ITS PYRIDINIUM ANALOGS[a]

Compound	k (sec^{-1})	pK_a[b]
cn⁴PdAD+	6.86×10^{-3} (1.83×10^{-5})[c]	2.14
β-NAD+	1.10×10^{-3} (4.83×10^{-7})	3.33
α-NAD+	2.80×10^{-4}	3.33
iNAD+	4.88×10^{-4} (7.97×10^{-8})	3.87
f⁴PdAD+	2.93×10^{-4}	4.72
PdAD+	1.66×10^{-5} (2.97×10^{-9})	5.23
n³PdAD+	3.11×10^{-6} (1.14×10^{-9})	5.98
((3,4-CH_3)$_2$)PdAD+	1.06×10^{-6}	6.48

[a] Determined in 50 mM sodium phosphate buffer at pH 6.4 and 100°C.

[b] pK_a of the parent pyridinium ion.

[c] Rate constants extrapolated at 37°C are shown in parentheses. The first-order rate constants were determined at three different temperatures (varying from 120 to 65°C) depending on the analog; the constant at 37°C was calculated from the Arrhenius equation.

three half-lives ($r > 0.99$). As noted before (*29*), once formed ADP–ribose was much less stable and it was gradually degraded into 5′-AMP and adenosine. The observed rates plotted according to Brönsted gave a linear relationship (Fig. 2) over 4.5 pK_a units: $\log k = -0.91\ pK_a - 0.0267$ ($r = 0.99$), with a slope $\beta_{lg} = -0.91$.

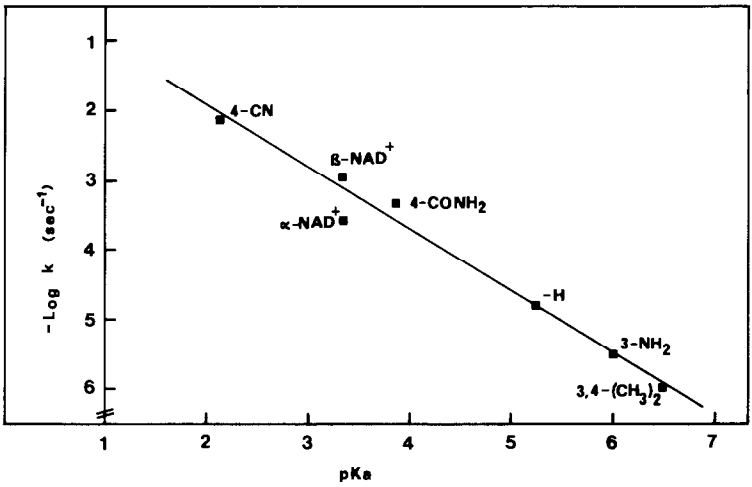

FIG. 2. Brönsted plot of the nonenzymatic hydrolysis of NAD+ and its analogs. The first-order hydrolysis rates, determined at 100°C in a 50 mM sodium phosphate buffer, pH 6.4, containing 0.5 M NaCl, are plotted against the pK_a of the leaving pyridine.

The hydrolysis rate constants were measured similarly at different temperatures and, using the Arrhenius relation, extrapolated to 37°C; in this case the slope of the Brönsted plot was -1.11 ($r = 0.99$). The rate of hydrolysis rate of the α-anomer of NAD^+ was also determined and it was found to be cleaved four times slower than β-NAD^+ at pH 6.4. Such a result is in sharp contrast with the data obtained at alkaline pH, where β-NAD^+ hydrolysis is two orders of magnitude faster than that of α-NAD^+ (Schuber and Oppenheimer, unpublished). It might be appropriate to mention here that α-NAD^+ is cleaved very slowly by calf spleen NAD^+ glycohydrolase: $V_\beta/V_\alpha = 10^4$ (C. Tarnus, unpublished).

DISCUSSION

The pyridine analogs of NAD^+ lacking a carbonyl function at position C-3 of the pyridinium moiety were found to be relatively poor substrates of calf spleen NAD^+ glycohydrolase. Their maximal rates of hydrolysis were determined in the present study and contrary to the good substrates (*5*), they proved very sensitive to the pK_a value of the departing pyridine. No large differences in binding energy of the analogs were observed, i.e., $K_i = 10 \pm 2$ μM; therefore the specificity of the enzyme cannot be correlated with specific interactions of the pyridinium substituents with the enzyme active site, but is attributable to the dynamic steps following the Michaelis complex formation. A linear relationship was found between the log of hydrolysis rate and the pK_a of the parent pyridines (Fig. 1), indicating that the cleavage of the pyridinium–ribose bond of the NAD^+ analogs was catalyzed by calf spleen NAD^+ glycohydrolase according to a single reaction mechanism over a 10^3 rate difference. Accordingly, the use of these pseudosubstrates allowed us to manipulate the kinetic parameters of the reaction process such that the chemical step of bond breaking became the rate-determining step. This contrasts with the NAD^+ glycohydrolase-catalyzed hydrolysis of NAD^+ where the rate-limiting step does not involve any covalency change and most probably reflects a transconformation of the Michaelis complex occurring before the actual nicotinamide–ribose bond-breaking step (*4, 5*). Our results are of importance because we now have the proper tools to study the thermodynamic and mechanistic aspects of the chemical reaction catalyzed by NAD^+ glycohydrolase, and the determination of the isotope effect on the hydrolysis of a slow-substrate should yield interesting information.

In our previous study we have speculated that a specific interaction between a carbonyl group at position C-3 of the pyridinium ring and the active site of the NAD^+ glycohydrolase was responsible for the slow transformation of the Michaelis complex (E.S) into a catalytically active complex (E·S)* in which the substrate is more destabilized (*5*). The analogs lacking this substituent would not benefit from such an effect, hence their slow rate of hydrolysis. The present work enabled us to estimate the energy involved in the observed increased catalytic efficiency; interpolation from the Brönsted plot indicates that NAD^+ is hydrolyzed 14 times faster than expected from the pK_a of nicotinamide ($\delta\Delta G‡ = -1.65$ kcal mol^{-1} at 37°C). This difference between the activation energies was some-

what higher, i.e., −2.28 kcal mol^{-1}, when calculated from the Hammett plot; however, such estimations rely heavily on a single substituent constant, e.g., the σ_m of the carboxamide group. The conclusion which we can reach, however, is that an apparent modest difference in energy barrier (about 2 kcal mol^{-1}) is sufficient to confer to the NAD$^+$ glycohydrolase a kinetic specificity and to mask in the hydrolysis of NAD$^+$ the barrier of the bond-breaking step. NMN$^+$, which lacks the adenosine 5′-phosphate subsite binding moiety (*32*), binds poorly to the active site of the enzyme (K_m = 1.3 mM), but its maximal rate of hydrolysis was still somewhat faster than expected from the energy of its nicotinamide–ribose bond. In this case the gain in activation energy is reduced to about $\delta\Delta G‡ = -1.0$ kcal mol^{-1}. It seems intriguing that such small shifts in energy barriers can result in the occurrence of secondary kinetic isotope effects (NMN$^+$) or in their total absence (NAD$^+$) as observed by Cordes' group (*4*). In fact our present knowledge of the kinetic mechanism of NAD$^+$ glycohydrolase gives access only to global kinetic barriers, i.e., in the case of NAD$^+$ hydrolysis: transconformation and bond breakage, and not to individual steps (*5*). It seems reasonable to assume that an efficient destabilization of, e.g., the nicotinamide–ribose bond in the (E·S)* complex, induced by a specific interaction, necessitates an energy cost which might be reflected by the slow transconformation of the Michaelis complex; therefore, the intrinsic energy gain in the pyridinium–ribose bond cleavage provided by the catalytically more active complex (E·S)* might be underestimated.

The important consequence of the Brönsted plot established here for the NAD$^+$ glycohydrolase-catalyzed reactions is the unequivocal information it gives on the mechanism of the pyridinium–ribose bond-breaking process. The slope of this plot has a highly negative value ($\beta_{lg} = -0.9$); this reflects a high sensitivity of the reaction to electronic factors and indicates that an electron deficiency is developing at the reaction center when going to the transition state. The magnitude of the slope is indicative of a late transition state, i.e., a large degree of bond breaking to the leaving group. These features are typical of a monomolecular decomposition mechanism of the pyridinium–ribose bond, generating an ADP–ribosyl oxocarbonium ion intermediate via a transition state possessing a closely related stereoelectronic structure. Indeed, under conditions where unimolecular decomposition (pH independent) is prevalent, nonenzymatic hydrolysis of pyridinium analogs of NAD$^+$ and of β-D-galactopyranosylpyridinium ions gave linear Brönsted plots with respectively $\beta_{lg} = -1.1$ (this work; see below) and −1.26 (*33*). Similar conclusions on the open nature of the transition state were reached in studies of spontaneous hydrolysis of other glycosylpyridinium (*34*) or methoxymethyl *N,N*-dimethylanilinium derivatives (*12*). In contrast, dealkylation of pyridinium derivatives according to a concerted nucleophic displacement (S_N-2 mechanism) are characterized by much smaller β_{lg} (*35, 36*). It results that for the NAD$^+$ glycohydrolase-catalyzed pyridinium–ribose bond breaking, the kinetic α-secondary isotope effects and the linear free-energy relationships observed with the rates of hydrolysis yield converging evidence in favor of a unimolecular reaction mechanism which proceeds via the formation, in the transition state, of a species presenting oxocarbonium ion character. In this context it is interesting to mention that similar results were obtained by Sinnott's group, with reactions catalyzed by

the β-galactosidase from *Escherichia coli*. Whereas the kinetic parameters k_{cat} and K_m showed no simple dependence on the aglycone acidity of aryl β-D-galactosylpyranosides, the rates of hydrolysis of poorer substrates such as β-D-galactopyranosylpyridinium salts were well correlated with the pK_a of the leaving pyridines (*37*).

The rates of nonenzymatic hydrolysis of pyridinium analogs of NAD^+ were also studied under experimental conditions favoring unimolecular decomposition. The ease of rupture of the pyridinium–ribose bond increases with electron-withdrawing substituents on the pyridinium moiety. The Brönsted plot was linear ($r = 0.99$) and $\beta_{lg} = -1.11$ when the observed rates were extrapolated to 37°C. Similar considerations as developed above for the enzyme-catalyzed reaction can be given to the significance of this value with regard to the structure of the transition state occurring during the hydrolytic cleavage of the C–N bond. Here again our data are consistent with the interpretation of the kinetic α-secondary deuterium effects measured for the spontaneous hydrolytic cleavage of β-NAD^+ (*4*).

At this stage of the discussion it might be relevant to compare the reaction pathways of the enzymatic and nonenzymatic processes. It seems obvious that NAD^+ glycohydrolase catalyzes the hydrolytic C–N bond cleavage of NAD^+, and its analogs, by accelerating a spontaneous chemical process; i.e., there is no evidence for a significant nucleophilic assistance by catalytic groups of the enzyme to pyridine departure. The slightly higher value of β_{lg} obtained for the nonenzymatic reaction is consistent with a "Hammond effect"; i.e., the amount of bond cleavage in the transition state is smaller in the enzyme-catalyzed reaction, the fastest one, therefore the structure of the transition state occurring along the pathway of the nonenzymatic reaction is closer to the oxocarbonium ion intermediate. Since the ribosyl oxocarbonium ion generated by the departure of the pyridine moiety is highly unstable, its occurrence as a free, solvent-equilibrated intermediate in the nonenzymatic reaction is questionable (*12, 38*). According to considerations developed by Jencks and co-workers (*9, 12, 38, 39*) the spontaneous hydrolysis of NAD^+ and its analogs could follow a preassociative mechanism where H_2O, the final nucleophilic acceptor, reacts in a solvent cage, the transition state being an open structure close to an oxocarbonium ion which is weakly stabilized both by the leaving pyridine and incipient solvent molecules. The entropy of activation, $\Delta S^{\ddagger} = -9.0$ cal $°K^{-1}$ mol^{-1}, measured for the hydrolysis of NAD^+, is consistent with such a proposal. The situation is somewhat different for the intermediate occurring in the enzyme-catalyzed reaction. From a structural point of view there now seems to be little doubt that a species resembling an oxocarbonium ion is generated by the C–N bond-breaking process. However, the intermediate formed must be stabilized by the active site of the enzyme since the departing pyridine must diffuse somewhat out of the active site in order for the E·ADP–ribosyl intermediary complex to be able to react with acceptors such as methanol or free pyridines, exclusively with retention of configuration (*7*). Moreover, such a stabilization, by decreasing the energy barrier of the pyridinium–ribose bond breaking, would be part of the catalytic process of the enzyme. In favor of this interpretation we have previously shown that the E·ADP–ribosyl intermediate reacts with methanol about 2 orders of magnitude faster than with

water (*7*); such a selectivity can only be observed with stabilized oxocarbonium ion intermediates, since highly reactive oxocarboniums, including those derived from glucosides, show no such preference (*39, 40*). An electrostatic stabilization, with more or less bond order, could in principle be provided by a carboxylate which would shield the α-face of the oxocarbonium for nucleophilic attack; such a residue was shown to be present in the active site of the NAD+ glycohydrolase (*32*). In the case of glycosidases some authors have favored the collapse of the oxocarbonium ion intermediates into an acylal (*33, 41*). Such covalent species are, however, relatively unreactive (*42*) and must revert back into an oxocarboniumlike ion in order to be trapped by acceptor molecules (*38*). For that reason for NAD+ glycohydrolase, where the reaction of the intermediary E·ADP–ribosyl with water or other acceptors is fast, we do not favor such an intermediate.

REFERENCES

1. PEKALA, P. H., AND ANDERSON, B. M. (1982) *in* The Pyridine Nucleotide Coenzymes (Everse, J., Anderson, B., and You, K., Eds.), pp. 325–377, Academic Press, New York.
2. ZATMAN, L. J., KAPLAN, N. O., AND COLOWICK, S. P. (1953) *J. Biol. Chem.* **200,** 197–212.
3. YUAN, J. H., AND ANDERSON, B. M. (1973) *J. Biol. Chem.* **248,** 417–421.
4. BULL, H. G., FERRAZ, J. P., CORDES, E. H., RIBBI, A., AND APITZ-CASTRO, R. (1978) *J. Biol. Chem.* **253,** 5186–5192.
5. SCHUBER, F., TRAVO, P., AND PASCAL, M. (1979) *Bioorg. Chem.* **8,** 83–90.
6. SCHUBER, F., TRAVO, P., AND PASCAL, M. (1976) *Eur. J. Biochem.* **69,** 593–602.
7. PASCAL, M., AND SCHUBER, F. (1976) *FEBS Lett.* **66,** 107–109.
8. KAPLAN, N. O., AND CIOTTI, M. (1956) *J. Biol. Chem.* **221,** 823–832.
9. JENCKS, W. P. (1980) *Acc. Chem. Res.* **13,** 161–169.
10. CRAZE, G. A., KIRBY, A. J., AND OSBORNE, R. (1978) *J. Chem. Soc. Perkin Trans. 2,* pp. 357–368.
11. FERRAZ, J. P., BULL, H. G., AND CORDES, E. H. (1978) *Arch. Biochem. Biophys.* **191,** 431–436.
12. KNIER, B. L., AND JENCKS, W. P. (1980) *J. Amer. Chem. Soc.* **102,** 6789–6798.
13. KIRSCH, J. F. (1972) *in* Advances in Linear Free Energy Relationships (Chapman, N. B., and Shorter, J., Eds.), pp. 369–400, Plenum, New York.
14. COOK, P. F., AND CLELAND, W. W. (1981) *Biochemistry* **20,** 1797–1805.
15. PARKIN, D. W., AND SCHRAMM, V. L. (1984) *J. Biol. Chem.* **259,** 9418–9425.
16. WALTER, P., AND KAPLAN, N. O. (1963) *J. Biol. Chem.* **238,** 2823–2830.
17. ZATMAN, L. J., KAPLAN, N. O., COLOWICK, S. P., AND CIOTTI, M. (1954) *J. Biol. Chem.* **209,** 467–484.
18. FISHER, T. L., VERCELLOTTI, S. V., AND ANDERSON, B. M. (1973) *J. Biol. Chem.* **248,** 4293–4299.
19. MULLER, C. D., TARNUS, C., AND SCHUBER, F. (1984) *Biochem. J.* **223,** 715–721.
20. KAPLAN, N. O., AND STOLZENBACH, F. R. (1957) *in* Methods in Enzymology, Vol. 3, pp. 899–905, Academic Press, New York.
21. OPPENHEIMER, N. J., *in* The Pyridine Nucleotide Coenzymes (Everse, J., Anderson, B., and You, K. S., Eds.), pp. 51–89. Academic Press, New York.
22. BIELLMANN, J. F., AND JUNG, M. J. (1970) *FEBS Lett.* **7,** 199–200.
23. SCHUBER, F., MULLER, H., AND SCHENHERR, I. (1980) *FEBS Lett.* **109,** 247–251.
24. PIETTA, P., PLACE, M., AND MENEGUS, F. (1983) *Anal. Biochem.* **131,** 533–537.
25. SCHUBER, F., AND TRAVO, P. (1976) *Eur. J. Biochem.* **65,** 247–255.
26. WILKINSON, G. W. (1961) *Biochem. J.* **80,** 324–332.
27. YOST, D. A., AND ANDERSON, B. M. (1982) *J. Biol. Chem.* **257,** 767–772.
28. CHAKRABARTY, M. R., HANDLOSER, C. S., AND MOSHER, M. W. (1973) *J. Chem. Soc. Perkin Trans. 2* pp. 938–942.

29. KAPLAN, N. O., COLOWICK, S. P., AND CARR BARNES, C. (1951) *J. Biol. Chem.* **191,** 461–472.
30. ANDERSON, B. M., AND ANDERSON, C. D. (1963) *J. Biol. Chem.* **238,** 1475–1478.
31. LOWRY, O. H., PASSONEAU, J. V., AND ROCK, M. K. (1961) *J. Biol. Chem.* **236,** 2756–2759.
32. SCHUBER, F., PASCAL, M., AND TRAVO, P. (1978) *Eur. J. Biochem.* **83,** 205–214.
33. JONES, C. C., SINNOTT, M. L., AND SOUCHARD, I. J. L. (1977) *J. Chem. Soc. Perkin II,* pp. 1191–1198.
34. HOSIE, L., MARSHALL, P. J., AND SINNOTT, M. L. (1984) *J. Chem. Soc. Perkin Trans. 2,* pp. 1121–1131.
35. BERG, U., GALLO, R., AND METZGER, J. (1976) *J. Org. Chem.* **41,** 2621–2624.
36. ARNETT, E. M., AND REICH, R. (1980) *J. Amer. Chem. Soc.* **102,** 5892–5902.
37. SINNOTT, M. L., AND WITHERS, S. G. (1974) *Biochem. J.* **143,** 751–762.
38. YOUNG, P. R., AND JENCKS, W. P. (1977) *J. Amer. Chem. Soc.* **99,** 8238–8248.
39. SINNOTT, M. L., AND JENCKS, W. P. (1980) *J. Amer. Chem. Soc.* **102,** 2026–2032.
40. RICHARD, J. P., AND JENCKS, W. P. (1984) *J. Amer. Chem. Soc.* **106,** 1373–1383.
41. ROSENBERG, S., AND KIRSCH, J. F. (1981) *Biochemistry* **20,** 3189–3196.
42. PAYNE, D. M., JACOBSON, E. L., MOSS, J., AND JACOBSON, M. K. (1985) *Biochemistry* **24,** 7540–7549.